

The Mechanism of Reaction of Fully Reduced Membrane-Bound Cytochrome Oxidase with Oxygen at 176K

By G. MARIUS CLORE* and EDWIN M. CHANCE

Department of Biochemistry, University College London, Gower Street, London WC1E 6BT, U.K.

(Received 30 August 1977)

1. The results of non-linear optimization studies on the mechanism of reaction of fully reduced cytochrome oxidase with O_2 at 176 K are presented. The analysis is carried out on data obtained by means of dual-wavelength multi-channel spectroscopy at three wavelength pairs (604–630, 608–630 and 830–940 nm) and at three O_2 concentrations (60, 200 and 1180 μM). The only model that satisfies the triple requirement of a standard deviation within the standard error of the experimental data, good determination of the optimized parameters and a random distribution of residuals is a three-species sequential mechanism. 2. On the basis of the optimized values of the relative absorption coefficients of the intermediates at each wavelength obtained from the present paper together with data from low-temperature trapping, e.p.r. and magnetic-susceptibility studies, the possible valence states of the metal centres in each of the intermediates are discussed.

The cytochrome oxidase complex (EC 1.9.3.1) catalyses the terminal reaction (i.e. the reduction of O_2 to water) in the respiratory electron-transport chain of all higher organisms, animals and plants, and also of the yeasts, algae and some bacteria. The minimum functioning unit of the mammalian cytochrome oxidase complex is thought to contain four metal centres consisting of two haems, a and a_3 , and two copper atoms, and varying amounts of phospholipid (Lemberg, 1969; Caughey *et al.*, 1976), part of which appears to be essential for its full enzymic activity (Awashti *et al.*, 1970).

The development of multi-channel spectroscopy (Chance *et al.*, 1975a) and a low-temperature kinetic method, known as triple trapping (Chance *et al.*, 1975b), for the flash photolysis of membrane-bound cytochrome oxidase with CO in the presence of O_2 , has led to the identification of two spectroscopically distinct species A_1 and B in the reaction of fully reduced cytochrome oxidase with O_2 (Chance *et al.*, 1975c,d). The rationale behind such low-temperature studies is that the energies of activation of the terminal reactions of the respiratory chain increase with the sequence of steps in the chain. The initial reactions with O_2 are of lower activation energy, and lowering the temperature makes them relatively faster than the oxidation of later components of the chain such as cytochrome c , thereby allowing intermediates to accumulate.

Compound A_1 was trapped at 176 K, and had an absorption spectrum with a peak at 591 nm and a trough at 611 nm; compound B was trapped at 203 K, and had a trough at 606 nm and no peak.

Abbreviation used: m.c.d., magnetic circular dichroism.

* To whom correspondence should be addressed.

No significant changes in the e.p.r. or optical signals were observed in the formation of compound A_1 , which was distinct from the CO compound on account of small but significant differences in the positions and intensities of their absorption bands, and very large differences in kinetic and equilibrium constants (with respect to fully reduced cytochrome oxidase) and in photosensitivity. It was recognized as functional by its inherent instability and ready conversion into compound B. The linear relationship between O_2 concentration and the rate of formation of compound A_1 , explored from $2 \times 10^6 M^{-1} \cdot s^{-1}$ at 245 K to $685 M^{-1} \cdot s^{-1}$ at 179 K, suggested that it was the first intermediate in the cytochrome oxidase- O_2 reaction. The formation of compound B was associated with a decrease in absorbance at 604 and 608 nm, an increase in absorbance at 830 nm and an increase in the e.p.r. signals of iron at $g = 3.05$ and copper at $g = 2.03$, suggesting oxidation of iron and copper components (Chance *et al.*, 1975c,d).

The present paper concerns the elucidation of the kinetics, mathematical symbolism and chemistry of the elementary steps of the reaction of fully reduced membrane-bound cytochrome oxidase with O_2 at 176 K by means of non-linear stiff numerical-integration techniques (Gear, 1971) to reconstruct the experimental traces, and non-linear optimization procedures (Powell, 1965, 1972) to evaluate the adequacy of fit of a given mechanism to the experimental data and the determination of the optimized parameters. The experimental data were obtained by means of dual-wavelength multi-channel spectroscopy (Chance *et al.*, 1975a) at three wavelength pairs (604–630, 608–630 and 830–940 nm) and at three O_2 concentrations (60, 200 and 1180 μM).

Experimental

Biochemical methods

Bovine heart mitochondria, prepared by the method of Low & Vallin (1963), are suspended at 298 K in a medium containing 0.2 M mannitol, 0.75 M sucrose, 50 mM sodium phosphate buffer, pH 7.2 at 198 K, 10 mM succinate and 10 mM glutamate, and left for 10 min (i.e. until all the O₂ in the preparation is exhausted). Control experiments with Phenol Red as a pH indicator demonstrated that no significant changes in pH occur on lowering the temperature to 143 K owing to the large buffering capacity of the high concentrations of protein in the preparation. The large buffering capacity of high concentrations of protein at sub-zero temperatures has also been observed by William-Smith *et al.* (1977). The system is then cooled to 273 K and saturated with 100% CO at 0.1 MPa (1 atm) for 10 min. Ethylene glycol is added (final concn. 30%, v/v) and the preparation is resaturated with 100% CO for a further 20 min to ensure full anaerobiosis and CO saturation. The concentration of CO in the CO-saturated preparation is 1.2 mM (Chance *et al.*, 1975b). The final concentration of mitochondria is 15 mg/ml, which contains 5 μM cytochrome oxidase calculated from $\epsilon_{\text{red.ox.}, 605} = 24.0 \text{ mm}^{-1} \cdot \text{cm}^{-1}$ (Van Gelder, 1963). The preparation is then stored in an air-tight syringe at 252 K until used. A sample (1 ml) of the reduced CO-saturated preparation is injected into a 2 mm light-path cuvette and O₂ (delivered as O₂ or air-saturated ethylene glycol) is introduced in the dark. Ethylene glycol saturated with O₂ at 250 K contains 2.0 mM-O₂ and at 296 K contains 1.2 mM-O₂; ethylene glycol saturated with air at 296 K contains 0.24 mM-O₂ (B. Chance, unpublished work). The cuvette is transferred to an ethanol/solid CO₂ bath at 195 K and the suspension stirred vigorously in the dark until the viscosity increases and freezing occurs. This procedure prevents ligand exchange between O₂ and the CO-inhibited system (Chance *et al.*, 1975b,c,d). The cuvette is then transferred to the Dewar flask of the spectrophotometer through which thermo-regulated N₂ of the desired temperature flows. A thermocouple of gold/cobalt alloy and copper inside the cuvette is used for temperature measurements. The reaction is activated at 176 K by a laser flash from a 0.1 J Rhodamine 6G dye laser that has a wavelength of 585 nm and a pulse width of 1 μs.

The temperature of 176 K was chosen for the following reason. Owing to the turbidity of the mitochondrial suspension the signal-to-noise ratio is too low, at times less than 0.1 s, to obtain meaningful data. Therefore we chose a temperature at which the reaction proceeded at an optimum rate for monitoring at the time resolution available. It is noteworthy that any temperature in the 173–178 K range could have been used (Chance *et al.*, 1975c,d).

Further, at higher temperatures cytochrome *c* oxidation occurs (Chance *et al.*, 1977; Denis, 1977), further complicating the system under consideration.

Biophysical methods

The spectrophotometric data recorded before, during and after the laser flash consists of two time-sharing Johnson Foundation multi-channel dual-wavelength spectrophotometers (Chance *et al.*, 1975a), one affording wavelengths appropriate to haem kinetics in the region of the α -band, and the other appropriate to i.r.-absorbance changes attributable to the kinetics of the copper components of cytochrome oxidase. The wavelengths of light are isolated by filters of appropriate spectral intervals and are interlaced, one with another, at intervals of 8 ms by synchronized 60 Hz rotating discs. The transmitted light is monitored with a multi-alkali photomultiplier for the 400–700 nm range (EMI 9592b) and a silicon diode detector for the 800–1000 nm range (United Detector Technology PIN-10). Thus all the data at each O₂ concentration are recorded simultaneously from the same sample at the same temperature with a single laser flash. The laser flash itself is approximately 99% saturating and the residual is not dissociated (Chance *et al.*, 1975d). CO does not recombine to a detectable extent in the presence of the relatively high concentrations of O₂ used (Chance *et al.*, 1975d).

Spectroscopic recordings and data digitization

At 176 K, the kinetics of formation of compound A₁ have a half-time of a few seconds, and thus can be resolved with an amplifier rise time of approx. 0.1 s. The kinetics were recorded on strip charts for a period of 320 s. Experimental data are digitized by the method described in Appendix 1. Fig. 1 shows the percentage absorbance change at the three wavelength pairs (604–630, 608–630 and 830–940 nm) and at three O₂ concentrations (60, 200 and 1180 μM) plotted as a function of time. The overall standard error of the data, given by the weighted mean of the standard errors of the individual spectroscopic curves, is $2 \pm 0.26\%$.

Numerical techniques

The numerical results of non-linear optimizations were obtained by using a computer program, FACSIMILE (Curtis & Chance, 1972; Curtis, 1976; Curtis & Kirby, 1977), which uses Gear's (1971) method for the numerical integration of large systems of simultaneous non-linear stiff ordinary differential equations. Optimization is carried out by a method developed by Powell (1965, 1972) that produces rapid convergence of the sum squares of

residuals for non-linear systems without calculating derivatives.

The residuals, the sum of whose squares is minimized, are computed as:

$$R_{ij} = [v_{ij} - (u_{ij}/s_i)]/\sigma_i \quad (1)$$

where *j* identifies the time point and *i* the data curve, *v_{ij}* is the observed value, *u_{ij}* the corresponding calculated value, *s_i* a scale factor and *σ_i* the standard error for curve *i*. The overall standard error of the data (*φ*) is given by the weighted mean of the standard error for each curve:

$$\phi = \sum(\sigma_i r_i) / \sum r_i \quad (2)$$

where *r_i* is the range of curve *i*.

The residual sum squares (RSQ) is given by:

$$RSQ = \sum_i^n \sum_{j=1}^m R_{ij}^2 \quad (3)$$

where *m* is the number of time points for each curve *i*, and *n* is the number of curves. At the minimum, RSQ is equal to chi-squared (*χ*²). Because the RSQ depends on the number of experimental points, the standard deviation is calculated:

$$s.d. = \phi[RSQ/(d-p)]^{1/2} \quad (4)$$

where *d* is the total number of experimental points and *p* the number of optimized parameters.

A quantitative measure of how accurately an unknown parameter has been determined by optimization is given by the standard deviation of the natural logarithm (s.d._{ln}) of the unknown parameter. Since rate constants and other parameters need to be varied over a large range of values, the natural logarithm of the unknown parameter is varied, and, consequently, the s.d._{ln} is calculated from the non-linear covariance. Because of the linearity of logarithms less than 0.2, a parameter whose s.d._{ln} lies below this value has a relative standard deviation of ±s.d._{ln} and is considered to have a well-determined minimum in multi-dimensional parameter space. For larger values of s.d._{ln} up to 1 in magnitude, the parameter value is determined to within a factor of *e* ≈ 2.72, and so its order of magnitude is known. Significantly larger values of s.d._{ln} show that the observations are inadequate to determine the parameter.

A measure of the nature of the distribution of the residuals is given by the correlation index (*C_j*):

$$C_j = \left(\frac{\sum_1^m R_j}{\sum_1^m R_j^2} \right)^{1/2} \quad (5)$$

If:

$$|C_j| \geq 1 \quad (6)$$

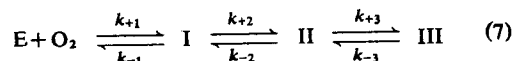
where a value of 1 is the expected root-mean-square value of *|C_j|* if the residuals were all independent random variables of zero mean and the same variance (see Appendix 3), the departures between calculated and observed curves are systematic and statistics such as *χ*² and the s.d., the variance-covariance matrix and

the s.d._{ln} of the optimized parameters have to be regarded with suspicion.

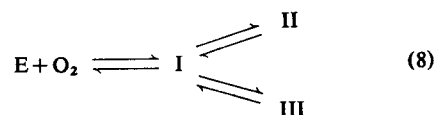
The choice of model in non-linear optimization problems depends, not only on obtaining an s.d. within the standard error of the experimental data, but also on obtaining a fit in which the optimized parameters are well determined and the distribution of residuals is random. This triple requirement greatly decreases the number of models available and provides a rigorous quantitative framework on which to base one's choice of model. For one model to be preferred over another it is necessary to demonstrate that, for an s.d. within the standard error of the data and a random distribution of residuals, one is able to obtain a better determination of the optimized parameters. Models with too many degrees of freedom will fail such an analysis because of under-determination, whereas models with too few degrees of freedom will fail such an analysis as a result of the introduction of systematic errors in the distribution of the residuals.

Results

Preliminary attempts at non-linear optimization of the coefficients of the differential equations representing a two-intermediate reaction system was found not to fit the data on the basis of s.d. (≥10%) and systematic errors in the distribution of residuals. This indicated the presence of other intermediates that had not been identified by low-temperature trapping and wavelength-scanning optical spectroscopy (Chance *et al.*, 1975c,d). The only model that satisfies the triple requirement of an s.d. within the standard error of the data (i.e. less than 2%), good determination of the optimized parameters and a random distribution of residuals, with no arbitrary constraints, is a three-species sequential mechanism, which is stated as follows:



where E is the fully reduced cytochrome oxidase complex and intermediate III the product of the reaction. Although more complicated models involving more intermediates and/or branching pathways are possible, the corresponding increase in the number of parameters that have to be optimized results in an under-determined system. Further, the only alternative model involving the same number of parameters is stated as:



and, like the two-intermediate reaction system, fails to fit the data on the basis of s.d. (≥10%) and systematic errors in the distribution of residuals.

The contribution of each intermediate to each wavelength is represented by a relative extinction coefficient. The crude absorbance at the i th wavelength, $W_i(t)$, in units of concentration, is given by:

$$W_i(t) = \sum_l F_l(t) \epsilon'_i(l) \quad (9)$$

where $F_l(t)$ is the concentration of the l th intermediate at time t and $\epsilon'_i(l)$ is the relative absorption coefficient of the l th intermediate at the i th wavelength.

On the basis of a qualitative interpretation of the data in Fig. 1 the following assignment of intermediates to each wavelength was made. The fully reduced cytochrome oxidase and intermediates I, II and III were assigned to the 604 and 608 nm traces:

$$W_{604} = [E] \epsilon'_{604}(E) + [I] \epsilon'_{604}(I) + [II] \epsilon'_{604}(II) + [III] \epsilon'_{604}(III) \quad (10)$$

$$W_{608} = [E] \epsilon'_{608}(E) + [I] \epsilon'_{608}(I) + [II] \epsilon'_{608}(II) + [III] \epsilon'_{608}(III) \quad (11)$$

The 830 nm traces were assigned to intermediates I, II and III:

$$W_{830} = [I] \epsilon'_{830}(I) + [II] \epsilon'_{830}(II) + [III] \epsilon'_{830}(III) \quad (12)$$

This is consistent with the idea that cupric copper makes the major contribution at this wavelength (Griffiths & Wharton, 1961; Wharton & Tzagaloff, 1963, 1964; Andreasson *et al.*, 1972; Aasa *et al.*, 1976; Wever *et al.*, 1977). Since the absorbance of fully reduced cytochrome oxidase (E) at 830–940 nm is zero (Chance & Leigh, 1977), E was not assigned to the 830 nm traces.

The crude computed absorbance, in units of concentration (given by eqn. 9), is converted into a percentage absorbance change ($N_i\%$) by means of a

scale factor and offset for the 604 and 608 nm traces, and a scale factor only for the 830 nm traces:

$$N_{604}\% = (W_{604} S_{604} - D_{604}) \times 100 \quad (13a)$$

$$N_{608}\% = (W_{608} S_{608} - D_{608}) \times 100 \quad (13b)$$

$$N_{830}\% = (W_{830} S_{830}) \times 100 \quad (13c)$$

where S_i are the scale factors and D_i the offsets. [The necessity for offsets in the case of the 604 and 608 nm traces is due to the fact that the last experimental point was given a value of zero, these traces being characterized by a decrease in absorption; however, the last experimental point does not correspond to a zero value of W_i and consequently an offset is required. In the case of the 830 nm traces, which are characterized by an increase in absorption, the first experimental point ($t = 0$ s) was given a value of zero; since W_{830} at $t = 0$ s is zero, no offset is required.]

In the initial optimization, all the following parameters were varied simultaneously.

(a) The rate constants $k_{+1}, k_{-1}, k_{+2}, k_{-2}, k_{+3}$ and k_{-3} .

(b) The relative absorption coefficients of intermediates I, II and III at 604 and 608 nm; these were varied relative to $\epsilon'_{604}(E)$ and $\epsilon'_{608}(E)$, the relative absorption coefficients of fully reduced cytochrome oxidase at 604 nm and 608 nm respectively, which were arbitrarily set to 1.0. The relative absorption coefficients of intermediates I and II at 830 nm; these were varied relative to $\epsilon'_{830}(III)$, the relative absorption coefficient of intermediate III, which was arbitrarily set to 1.0.

(c) The scale factors and offsets for each wavelength at each O_2 concentration ($S_{604A}, D_{604A}, S_{604B}, D_{604B}, S_{604C}, D_{604C}; S_{608A}, D_{608A}, S_{608B}, D_{608B}, S_{608C}, D_{608C}; S_{830A}, S_{830B}, S_{830C}$. The subscripts A, B and C refer to O_2 concentrations of 60, 200 and 1180 μM respectively.)

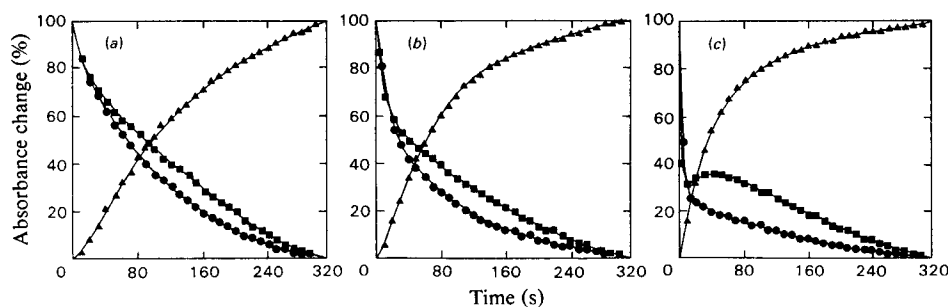


Fig. 1. Observed kinetics of the reduction of O_2 by fully reduced membrane-bound cytochrome oxidase at 176 K as measured at three wavelength pairs

Symbols: ●, 604–630 nm; ■, 608–630 nm; ▲, 830–940 nm. Theoretical curves are shown as solid lines. The experimental conditions are: bovine heart mitochondria, 15 mg/ml (containing 5 μM -cytochrome oxidase); 30% ethylene glycol; 0.2 M-mannitol; 0.75 M-sucrose, 50 mM-sodium phosphate buffer, pH 7.2; 10 mM-succinate; 10 mM-glutamate; 1.2 mM-CO; in the presence of 60 μM - O_2 (a), 200 μM - O_2 (b) and 1180 μM - O_2 (c).

All the parameters were well determined except for the rate constant k_{-3} , the relative absorption coefficients of intermediate III at 604 nm and 608 nm [$\epsilon'_{604}(\text{III})$ and $\epsilon'_{608}(\text{III})$], and the relative absorption coefficient of intermediate I at 830 nm [$\epsilon'_{830}(\text{I})$] whose values were both small and very poorly determined (s.d._{in} $\gg 10$), indicating that the value of these parameters is essentially zero. The small value and poor determination of k_{-3} indicates that the formation of intermediate III is essentially irreversible at 176 K. In the subsequent optimization k_{-3} was set to a suitably low value ($1 \times 10^{-6} \text{ s}^{-1}$), and $\epsilon'_{604}(\text{III})$, $\epsilon'_{608}(\text{III})$ and $\epsilon'_{830}(\text{I})$ were set to zero. In the resulting solution all the parameters were well determined. The values of the correlation indices for each curve, the mean absolute correlation index, χ^2 and the overall s.d. of the fit are shown in Table 1; the values of the optimized parameters together with their s.d._{in} and confidence limits are shown in Table 2. The comparison of the experimental traces and the computed curves is shown in Fig. 1.

Figs. 2 and 3 illustrate the kinetics of the individual intermediates and their relationship to the absorbance changes at 604–630, 608–630 and 830–940 nm. Starting just after photolysis of the CO-inhibited compound (at $t = 0$ s) the traces begin with the free reduced form of cytochrome oxidase at zero concentration of the intermediates. Intermediate I rises first to a plateau of 18, 38 and 73% of the total enzyme concentration at 60 μM -, 200 μM - and 1180 μM -O₂ respectively. Intermediate I is rapidly converted

into intermediate II, which rises to a later and larger maximum at 60 μM - and 200 μM -O₂ (36 and 52% respectively), and to a later but smaller maximum at 1180 μM -O₂ (62%). The reason for the low maxima of intermediates I and II is because of their rapid conversion into intermediate III, which is the final product of the reaction. This final intermediate shows an induction period in its formation together with a slow rise to its final plateau value characteristic of the product of an enzymic sequence. Table 3 shows the calculated values for the half-times of formation and disappearance of the intermediates at the three O₂ concentrations.

Discussion

General assumptions in the assignment of valence states of the four metal centres to the intermediates

In the following sections we attempt to assign valence states to the four metal centres of cytochrome oxidase in each of the intermediates. In doing so we recognize that it may be an oversimplification to assume that electrons are localized on particular metal centres rather than being distributed in some statistical manner among them.

Only two species, A₁ and B, have been trapped at low temperatures in the reaction of fully reduced membrane-bound cytochrome oxidase with O₂ and characterized by optical-wavelength scanning and e.p.r. spectroscopy (Chance *et al.*, 1975c,d). In the discussion below the following general assumptions about the relationship of these two species with the three kinetically identified intermediates of this study are made.

(1) Compound A₁ is equivalent to intermediate I. This seems reasonable, as Fig. 3 shows that, 10 s after flash photolysis, the time at which compound A₁ was trapped at 176 K (Chance *et al.*, 1975d), the concentration of intermediates II and III is insignificant relative to that of intermediate I. Similarly, compound A₂, the first species trapped in the reaction of mixed-valence-state cytochrome oxidase ($a_3^{2+}\text{Cu}^+ \cdot a_3^{3+}\text{Cu}^{2+}$) with O₂ (Chance *et al.*, 1975c,d) is equivalent to intermediate I_M (Clore & Chance, 1978), the justification being the same as that for intermediate I (Clore & Chance, 1978).

(2) Compound B is equivalent to intermediate III. This seems reasonable, since compound B is the stable end product of the reaction in the 173–195 K range (Chance *et al.*, 1977).

Therefore, in the discussion that follows, the first and third intermediates in the reaction of fully reduced cytochrome oxidase with O₂ are referred to as intermediates I and III rather than compounds A₁ and B respectively; similarly, the first intermediate in the reaction of mixed-valence-state cytochrome

Table 1. Values of the correlation indices for each curve, the mean absolute correlation index, χ^2 and the overall s.d.

The correlation index (C_i) is a measure of the distribution of residuals. For $|C_i| < 1.0$, the distribution of residuals is random; for $|C_i| \gg 1.0$, the deviations between the calculated and observed values are systematic. Mean absolute correlation index (\bar{C}) is

$$0.610 \left(\bar{C} = \frac{1}{k} \sum_{i=1}^k |C_i| \right), \text{ where } k \text{ is the number of curves.}$$

χ^2 is 245 for 272 degrees of freedom (297 observations and 25 parameters). For values of $f > 100$, where f is the number of degrees of freedom, the confidence limits for χ^2 are given by $\frac{1}{2}[(2f-1)^{\pm 1} (1 \pm \zeta z_{\alpha/2})]^2$, where $z_{\alpha/2}$ is the value of the standard normal variable at the $\alpha/2$ confidence level and ζ is the fractional error in the estimation of the overall standard error of the data (in this case 0.13). The 99% confidence interval for χ^2 at 272 degrees of freedom is 120–484. Overall s.d. is 1.9%. The overall standard error of the data is $2 \pm 0.26\%$ with a 99% confidence interval of 1.33–2.67%.

Wavelength (nm)	Correlation indices		
	60 μM -O ₂	200 μM -O ₂	1180 μM -O ₂
604–630	-0.694	-0.453	0.669
608–630	-0.321	-0.120	0.399
830–940	0.811	0.332	0.607

Table 2. Optimized values of the parameters together with their s.d._{in} and confidence limits

Parameter number	Parameter	Dimensions	Optimized value	s.d. _{in}	Confidence limits	
					5%	95%
1	k_{+1}	$M^{-1} \cdot s^{-1}$	310	0.149	242	396
2	k_{-1}	s^{-1}	0.0398	0.286	0.0248	0.0638
3	k_{+2}	s^{-1}	0.0321	0.108	0.0269	0.0383
4	k_{-2}	s^{-1}	0.00438	0.530	0.00183	0.0105
5	k_{+3}	s^{-1}	0.00532	0.152	0.00414	0.00683
6	k_{-3}	s^{-1}	1×10^{-6} *			
7	$\epsilon'_{604}(I)\dagger$		0.170	0.453	0.0805	0.358
8	$\epsilon'_{604}(II)\dagger$		0.196	0.219	0.137	0.281
9	$\epsilon'_{604}(III)\dagger$		0*			
10	$\epsilon'_{608}(I)\dagger$		0.252	0.232	0.172	0.369
11	$\epsilon'_{608}(II)\dagger$		0.521	0.0631	0.469	0.578
12	$\epsilon'_{608}(III)\dagger$		0*			
13	$\epsilon'_{830}(I)\dagger$		0*			
14	$\epsilon'_{830}(II)\dagger$		0.789	0.0918	0.678	0.917
15	S_{604A}	μM^{-1}	0.243	0.0735	0.215	0.274
16	D_{604A}		0.362	0.223	0.251	0.522
17	S_{604B}	μM^{-1}	0.217	0.0640	0.195	0.241
18	D_{604B}		0.0879	0.217	0.0615	0.126
19	S_{604C}	μM^{-1}	0.215	0.214	0.151	0.306
20	D_{604C}		0.0768	0.147	0.0603	0.0978
21	S_{608A}	μM^{-1}	0.279	0.0695	0.249	0.313
22	D_{608A}		0.397	0.168	0.301	0.523
23	S_{608B}	μM^{-1}	0.246	0.0427	0.229	0.264
24	D_{608B}		0.232	0.143	0.183	0.294
25	S_{608C}	μM^{-1}	0.236	0.0725	0.209	0.266
26	D_{608C}		0.179	0.176	0.134	0.239
27	S_{830A}	μM^{-1}	0.246	0.0640	0.221	0.273
28	S_{830B}	μM^{-1}	0.224	0.0276	0.214	0.234
29	S_{830C}	μM^{-1}	0.219	0.0185	0.212	0.226

* k_{-3} , $\epsilon'_{604}(III)$, $\epsilon'_{608}(III)$ and $\epsilon'_{830}(I)$ were constrained at these values on the basis of initial optimizations in which their values were small and very poorly determined (s.d._{in} ≥ 10).

† The relative absorption coefficients at 604, 608 and 830 nm are $\epsilon'_{604}(I)$, $\epsilon'_{608}(I)$ and $\epsilon'_{830}(I)$ respectively, where I is the intermediate referred to. The $\epsilon'_{604}(I)$ and $\epsilon'_{608}(I)$ were varied relative to $\epsilon'_{604}(E)$ and $\epsilon'_{608}(E)$ respectively, the absorption coefficients of fully reduced cytochrome oxidase at 604 and 608 nm, which were given a value of 1.0. The $\epsilon'_{830}(I)$ were varied relative to $\epsilon'_{830}(III)$, the relative absorption coefficient of intermediate III at 830 nm, which was given a value of 1.0.

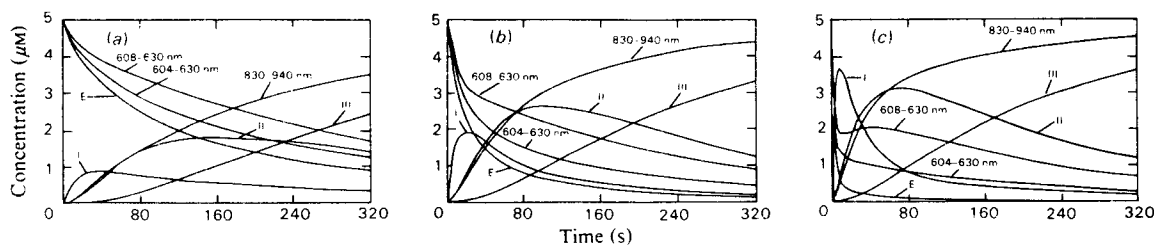


Fig. 2. Computed reaction kinetics of the individual intermediates and their relationship to the theoretical absorbance changes (in units of concentration) at 604–630 nm, 608–630 nm and 830–940 nm in the reaction of fully reduced membrane-bound cytochrome oxidase with O_2 at 176 K

The curves were obtained by numerical integration of the differential equations representing a three-intermediate sequential mechanism, by using the values of the rate constants and relative absorption coefficients obtained by optimization. Initial conditions: $5 \mu M$ -fully reduced cytochrome oxidase (E); in the presence of $60 \mu M-O_2$ (a), $200 \mu M-O_2$ (b) and $1180 \mu M-O_2$ (c).

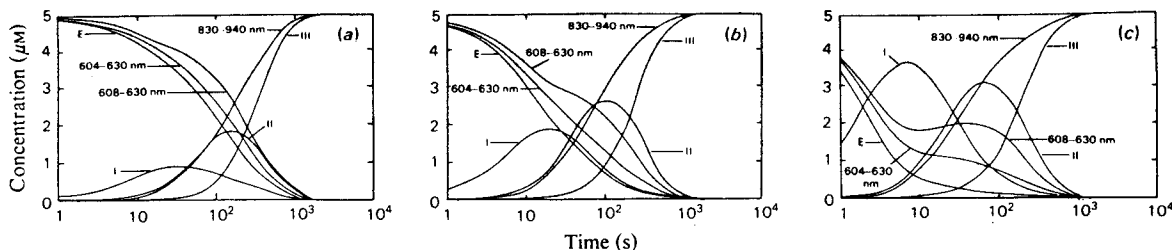


Fig. 3. Computed reaction kinetics of the individual intermediates and their relationship to the theoretical absorbance changes (in units of concentration) at 604–630 nm, 608–630 nm and 830–940 nm in the reaction of fully reduced membrane-bound cytochrome oxidase with O₂ at 176 K, plotted on a logarithmic time scale

The kinetics are shown up till the end point of the reaction. An estimate of the stiffness of this system is given by the ratio of the longest to the shortest time constant: the shortest time constant is $1/(332[\text{O}_2]) \geq 2.55$ s, and the longest is 10^6 s, giving a ratio of 3.92×10^5 . Initial conditions: $5 \mu\text{M}$ -fully reduced cytochrome oxidase (E) in the presence of $60 \mu\text{M-O}_2$ (a), $200 \mu\text{M-O}_2$ (b) and $1180 \mu\text{M-O}_2$ (c).

Table 3. Calculated half-times of formation ($t_{\frac{1}{2} \text{ on}}$) and disappearance ($t_{\frac{1}{2} \text{ off}}$) of the intermediates at $60 \mu\text{M}$, $200 \mu\text{M}$ - and $1180 \mu\text{M-O}_2$ at 176 K

	Fully reduced cytochrome oxidase	Inter-mediate I	Inter-mediate II	Inter-mediate III
$t_{\frac{1}{2} \text{ on}}$ (s) at:				
$60 \mu\text{M-O}_2$		6.31	44.7	317
$200 \mu\text{M-O}_2$		3.98	29.2	224
$1180 \mu\text{M-O}_2$		1.33	23.4	179
$t_{\frac{1}{2} \text{ off}}$ (s) at:				
$60 \mu\text{M-O}_2$	79.4	201	448	
$200 \mu\text{M-O}_2$	15.2	80.5	317	
$1180 \mu\text{M-O}_2$	2.00	36.5	252	

oxidase with O₂ inferred as intermediate I_M rather than compound A₂.

Further, the terms haem-haem, haem-copper and copper-copper interactions are used in their most general phenomenological sense, which is intended to include all mechanisms by which any modification in one of the metal components of cytochrome oxidase may affect the properties of the others.

Other assumptions will be made as they arise.

In the discussion that follows, we attempt to assign particular valence states to the haem and copper moieties in each intermediate on the basis of the optimized values of the relative absorption coefficients of the intermediates at each wavelength obtained from the present paper, the optical wavelength scanning and e.p.r. data on intermediates I and III (Chance *et al.*, 1975c,d) and the magnitude of the absorbance changes at 655 nm, a band attributed to interactions between haem a₃ and e.p.r.-undetectable copper (Beinert *et al.*, 1976; Palmer *et al.*,

1976), during the course of the reaction at low temperatures (Chance *et al.*, 1977; Denis, 1977). The reaction sequence, together with the optimized values of the relative absorption coefficients, rate constants and equilibrium constants at 176 K and the proposed valence states of the four metal centres in each intermediate, is summarized in Table 4.

Assignment of valence states of the copper atoms to the intermediates

In assigning particular valence states of the copper atoms to individual intermediates we make the following five assumptions.

(1) One copper atom, termed Cu_A, is e.p.r.-detectable with a signal around $g = 2$ (Beinert *et al.*, 1962; Beinert & Palmer, 1964; Van Gelder & Beinert, 1969; Malkin & Malmström, 1970; Aasa *et al.*, 1976) and magnetically isolated (Palmer *et al.*, 1976). The other copper atom, termed Cu_B, is undetectable by e.p.r. and antiferromagnetically coupled to haem a₃³⁺ when in the cupric state (Palmer *et al.*, 1976; Thomson *et al.*, 1976, 1977; Falk *et al.*, 1977).

(2) The e.p.r.-undetectable copper Cu_B becomes oxidized before the e.p.r.-detectable copper Cu_A. This seems reasonable in view of the higher midpoint redox potential of Cu_B, 340 ± 10 mV (Mackay *et al.*, 1973; Lindsay & Wilson, 1974; Lindsay *et al.*, 1975; Wilson *et al.*, 1975), compared with that of Cu_A, 245 ± 10 mV (Erecinska *et al.*, 1971; Wilson & Leigh, 1972).

(3) Cupric copper is the major contributor to the 830 nm traces. General agreement on the assignment of the i.r.-absorbance bands of cytochrome oxidase largely, if not completely, to the copper atoms in the cupric state seems confirmed (Aasa *et al.*, 1976; Wever *et al.*, 1977). The assignment of these bands

Table 4. Proposed chemical identity of the intermediates and the reaction sequence at 176 K, with the optimized values of the rate constants and relative absorption coefficients, and the calculated values of the equilibrium constants together with their S.D._{1n} and confidence limits

Reaction sequence and rate constants at 176 K	$O_2 + E \xrightleftharpoons[k_{-1}]{k_{+1}} I \xrightleftharpoons[k_{-2}]{k_{+2}} II \xrightleftharpoons[k_{-3}]{k_{+3}} III$			
Equilibrium constants (k_{+i}/k_{-i})	7949 M ⁻¹	7.33	5320	
correlation coefficient (r)	0.828	-0.698		
S.D. _{1n}	0.183	0.610		
5-95% confidence limits	5883-10740 M ⁻¹	2.69-20.0		
Relative extinction coefficients at:				
604-630 nm [$\epsilon'_{604}(I)$]	1.0 (73.2%)	0.170 (12.5%)	0.196 (14.3%)	0 (0%)
608-630 nm [$\epsilon'_{608}(I)$]	1.0 (56.4%)	0.252 (14.2%)	0.521 (29.4%)	0 (0%)
830-940 nm [$\epsilon'_{830}(I)$]	0 (0%)	0 (0%)	0.789 (44.1%)	1.0 (55.9%)
Proposed chemical identity of the intermediates*†	$a_3^{2+}Cu_B^+$ $a^2Cu_A^+$	$a_3^{3+}Cu_B^+$ $a^2Cu_A^+ \cdot O_2$	$a_3^{2+}Cu_B^{2+} \cdot O_2^{2-}$ $a^{3+}Cu_A^+ \cdot O_2^{2-}$	$a_3^?Cu_B^?$ $a^?Cu_A^{2+} \cdot O_2$

* Cu_A is e.p.r.-detectable copper and Cu_B is e.p.r.-undetectable copper.

† Since it is not known at present at what stage cleavage of the O-O bond occurs, whether cleavage is homolytic or heterolytic, and whether protonation takes place at this low temperature, the reduced O₂ species are represented as O₂^{x-} where x indicates the number of electrons donated to O₂.

to cupric copper is well founded on reductive titrations of fully oxidized cytochrome oxidase (Wever *et al.*, 1977).

(4) The two copper atoms of cytochrome oxidase make separate contributions to the absorbance at 830 nm just as do haem *a*₃ and haem *a* to the absorbance at 604 and 444 nm. Although one of the copper atoms, Cu_B, is undetectable by e.p.r., it seems unlikely that electron-spin pairing and antiferromagnetic coupling, which may be the cause of the invisibility of a portion of the e.p.r. signal caused by cupric copper, would at the same time cause the disappearance of the electronic transitions detected by optical spectroscopy. Also, the existence of separate contributions of the two copper atoms at 830 nm is further supported by the observation that significant increases in absorption take place at 830 nm in the reaction of ferricyanide-pretreated mixed-valence-state cytochrome oxidase ($a_3^{2+}Cu_B^+ \cdot a^3Cu_A^{2+}$) with O₂ (Chance & Leigh, 1977; Clore & Chance, 1978), where only e.p.r.-undetectable copper Cu_B can undergo oxidation, the e.p.r.-detectable copper Cu_A remaining in the cupric state throughout the reaction, as shown by the absence of any change in the intensity of the e.p.r. signal due to cupric copper at *g* = 2 during the course of the reaction (Chance & Leigh, 1977).

(5) Copper-haem and copper-copper interactions may affect the relative contributions of the two copper atoms at 830 nm, as suggested by Chance & Leigh (1977).

Tables 2 and 4 show that the 830 nm traces are best fitted by a 44% and 56% contribution from intermediates II and III respectively and no contribution from fully reduced cytochrome oxidase and intermediate I. Since there is no cupric copper in the fully reduced cytochrome oxidase we deduce, on the basis of the above assumptions, that there is no cupric copper in intermediate I. Since both intermediates II and III contribute to the absorbance at 830 nm, we deduce that they both contain cupric copper.

The increase in relative absorption coefficient of intermediate III with respect to that of intermediate II is highly significant [$\epsilon'_{830}(III) - \epsilon'_{830}(II) = 0.21 \pm 0.07$; also see Table 2]. This suggests three possibilities.

(i) In intermediate II, Cu_B is in the cupric state and Cu_A in the cuprous state, and in intermediate III Cu_B is in the cuprous state and Cu_A in the cupric state. The difference in the relative absorption coefficients of intermediates II and III at 830 nm is then attributed to the larger contribution of Cu_A²⁺ to the absorbance at 830 nm in intermediate III.

(ii) Intermediate II contains one atom of cupric copper, Cu_B²⁺, and intermediate III contains two atoms of cupric copper, Cu_B²⁺ and Cu_A²⁺.

(iii) In both intermediates II and III Cu_B is in the cupric state and Cu_A in the cuprous state, the difference in the relative absorption coefficients of intermediates II and III being attributed to the effects of copper-copper and/or copper-haem interactions on the absorbance at 830 nm.

Of these three possibilities, possibility (iii) can be

discounted by the observation that intermediate III exhibits an e.p.r. copper signal at $g = 2$, indicating that at least one copper atom, namely e.p.r.-detectable copper Cu_A, must be in the cupric state in intermediate III.

Assignment of valence states of haems a₃ and a to the intermediates

In assigning particular valence states of the iron atoms of the two haems, a₃ and a, to individual intermediates we make the following three assumptions:

(1) Haem-haem (Wikström *et al.*, 1976) and haem-copper interactions (Palmer *et al.*, 1976) may affect the relative contributions of haem a₃²⁺ and haem a²⁺ to the absorbance at 604 and 608 nm.

(2) Higher valence states of haem iron [i.e. Fe(IV) and greater] do not occur in the reaction of fully reduced cytochrome oxidase with O₂. Although higher valence states have been postulated for the low-temperature product of the reaction of ferricyanide-pretreated mixed-valence-state cytochrome oxidase with O₂ (Chance *et al.*, 1975c,d), there is no evidence from optical or e.p.r. spectroscopy for their existence in the reaction of fully reduced cytochrome oxidase with O₂ (Chance *et al.*, 1975c,d; Chance & Leigh, 1977). Therefore we will not consider higher valence states of iron in the following discussion.

Unlike our paper dealing with the kinetics of the reaction of ferricyanide-pretreated mixed-valence-state cytochrome oxidase with O₂ (Clore & Chance, 1978), we do not assume that a relative absorption coefficient of zero at both 604 and 608 nm imply that both haems are in the ferric state. The reason is two-fold. (a) At equilibrium virtually all the cytochrome oxidase will be in the form of intermediate III (see Fig. 3). Since no absorbance changes take place once equilibrium is reached, $\epsilon'_{604}(\text{III})$ and $\epsilon'_{608}(\text{III})$ will be poorly determined and no contribution at 604 and 608 nm from intermediate III will be required to fit the progress curves at 604 and 608 nm. (b) Chance *et al.* (1977) have demonstrated that, by the time equilibrium is reached in the 173–195 K range, only 40% of the total oxidized-reduced absorbance change at 605 nm (at the corresponding temperature) has taken place.

Table 2 shows that, within the errors specified, for the 604 nm traces:

$$\begin{aligned} \epsilon'_{604}(\text{E}) &> \epsilon'_{604}(\text{I}) \\ \epsilon'_{604}(\text{E}) &> \epsilon'_{604}(\text{II}) \\ \epsilon'_{604}(\text{I}) &= \epsilon'_{604}(\text{II}) \\ \epsilon'_{604}(\text{III}) &= 0 \end{aligned} \quad (14)$$

and for the 608 nm traces:

$$\begin{aligned} \epsilon'_{608}(\text{E}) &> \epsilon'_{608}(\text{II}) > \epsilon'_{608}(\text{I}) \\ \epsilon'_{608}(\text{III}) &= 0 \end{aligned} \quad (15)$$

The large decrease in the relative absorption coefficients of intermediate I with respect to fully reduced cytochrome oxidase at both 604 and 608 nm (see Tables 2 and 4) can be attributed either to a one-electron reduction of O₂ resulting in the production of a superoxide ion and the oxidation of haem a₃ to the ferric state (a₃³⁺·O₂⁻) or to ligand binding of O₂ without electron transfer to form an oxy compound of the ferrous haem (a₃²⁺·O₂). The latter view has been put forward by Chance *et al.* (1975c,d) on the basis of the similarity of the spectra of intermediate I and the fully reduced cytochrome oxidase-CO complex; however, these authors also point out that there are small but significant differences in both the positions and the intensities of their absorption bands. We favour the former view for the following reasons. Intermediate I_M, the first intermediate in the reaction of ferricyanide-pretreated mixed-valence-state cytochrome oxidase (a₃²⁺Cu_B⁺·a³⁺Cu_A²⁺) with O₂ (Chance *et al.*, 1975c,d; Clore & Chance, 1978), has a relative absorption coefficient of zero at both 604 and 608 nm relative to the mixed-valence-state oxidase, which strongly suggests that both haem a₃ and haem a are in the ferric state (Clore & Chance, 1978). Since the formation of intermediate I_M is not accompanied by an increase in absorption at 830 nm relative to the free initial mixed-valence-state cytochrome oxidase, it was deduced that it only involves a one-electron reduction of O₂, resulting in the oxidation of haem a₃ to the ferric state and the production of a superoxide ion (Clore & Chance, 1978). Haem-haem and haem-copper interactions in the formation of both intermediates I and I_M seem to be small. First, the kinetic and equilibrium parameters for the formation of intermediates I and I_M are very similar; secondly, the difference spectra of intermediates I and I_M with respect to fully reduced and mixed-valence-state cytochrome oxidase respectively are nearly the same, intermediate I having a peak at 591 nm, a shoulder at 600 nm and a trough at 611 nm, and intermediate I_M having a peak at 590 nm, a shoulder at 600 nm and a trough at 612 nm (Chance *et al.*, 1975c,d). Further, it seems likely that the slight differences in the optical spectra of intermediates I and I_M can be attributed to slightly different trapping conditions. This strongly suggests that both haem a₃ and O₂ are in the same configuration in intermediate I as in intermediate I_M, namely a₃³⁺·O₂⁻.

Further assignments of the valence states of the four metal centres in intermediates II and III

Any assignment of the valence states of the four metal centres must account for the observation that no 655 nm band is formed during the course of the reaction at temperatures below 195 K (Chance *et al.*, 1977; Denis, 1977). Beinert *et al.* (1976) have demonstrated that the weak absorption band at

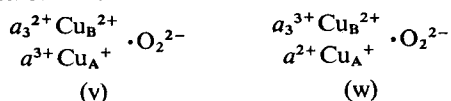
655 nm decreases in intensity during reductive titration as the ferric high-spin e.p.r. signals appear. A corresponding derivative-shaped curve has also been observed at 665 nm in the m.c.d. spectra (Babcock *et al.*, 1976). This has led to the suggestion that the 655 nm band arises as a consequence of anti-ferromagnetic coupling between high-spin haem a_3^{3+} and e.p.r.-undetectable copper, Cu_B^{2+} (Palmer *et al.*, 1976), evidence for such coupling coming from both n.m.r. (Falk *et al.*, 1977) and m.c.d. (Thomson *et al.*, 1976, 1977; Palmer *et al.*, 1976) studies.

Although the relative absorption coefficients of intermediates I and II are approximately equal at 604 nm, there is a highly significant increase in the relative absorption coefficient of intermediate II with respect to intermediate I at 608 nm [$\epsilon_{608}(\text{II}) - \epsilon_{608}(\text{I}) = 0.27 \pm 0.10$; also see Table 2]. This suggests two possibilities.

(i) An internal oxidation-reduction resulting in the oxidation of haem a to the ferric state and the reduction of haem a_3 to the ferrous state in intermediate II. The difference in the relative absorption coefficients of intermediates I and II is then attributed to the larger contribution of haem a_3^{2+} in intermediate II.

(ii) Haem a_3 remains in the ferric state and haem a in the ferrous state, the difference in the relative absorption coefficients of intermediates I and II being attributed to the effects of haem-haem and/or haem-copper interactions on the absorbance at 608 nm.

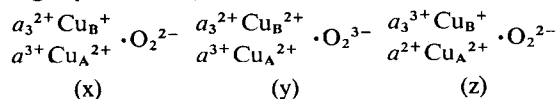
Thus there are two possible configurations for intermediate II:



Configuration (w), however, can be discounted on the basis that haem a_3^{3+} and Cu_B^{2+} would be expected to be anti-ferromagnetically coupled, and would therefore be expected to exhibit a 655 nm absorption band.

On the basis of the evidence presented so far, a basic scheme can be constructed, the first step involving a one-electron reduction of O_2 to the O_2^- state, and the second a one-electron reduction of O_2^- to the O_2^{2-} state. The valencies of haem a_3 , haem a and Cu_B , and the number of electrons donated to O_2 in intermediate III, are not specified.

The decrease in the relative absorption coefficients at 604 and 608 nm of intermediate III with respect to those of intermediate II could be accounted for by three possible configurations (discounting all those where anti-ferromagnetic coupling between high-spin haem a_3^{3+} and Cu_B^{2+} can occur):



The observation that intermediate III exhibits a low-spin ferric-haem e.p.r. signal at $g = 3.05$ but no high-spin ferric-haem e.p.r. signal at $g = 6$ (Chance *et al.*, 1975c,d, 1977) argues against configuration (z), where haem a_3^{3+} would be expected to be in the high-spin state. However, the definitive distinction between these three configurations will require careful Mössbauer and magnetic-susceptibility studies.

We thank Dr. B. Chance and Mr. A. R. Curtis for stimulating discussion, criticism and continual encouragement. We thank the Johnson Research Foundation for experimental facilities, and the University College London Computer Centre and the A.E.R.E. for computing facilities. G. M. C. acknowledges a Carlo Campolin Scholarship.

References

- Aasa, R., Albracht, S. P. J., Falk, K.-E., Lanne, B. & Vanngård, T. (1976) *Biochim. Biophys. Acta* **422**, 260-272
- Andreasson, L. E., Malmström, B. G., Stromberg, C. & Vanngård, T. (1972) *FEBS Lett.* **28**, 297-301
- Awashiti, Y. C., Chuang, F. F., Kleenan, T. W. & Crane, F. L. (1970) *Biochim. Biophys. Acta* **226**, 42-52
- Babcock, G. T., Vickery, L. & Palmer, G. (1976) *Biophys. J.* **16**, 87a
- Beinert, H. & Palmer, G. (1964) *J. Biol. Chem.* **239**, 1221-1227
- Beinert, H., Griffiths, D. E., Wharton, D. C. & Sands, R. H. (1962) *J. Biol. Chem.* **237**, 2337-2346
- Beinert, H., Hansen, R. E. & Hartzell, C. R. (1976) *Biochim. Biophys. Acta* **423**, 339-355
- Caughey, W. S., Wallace, W. J., Volpe, J. A. & Yoshikawa, S. (1976) *Enzymes 3rd Ed.* **13**, 299-344
- Chance, B. & Leigh, J. S. (1977) *Proc. Natl. Acad. Sci. U.S.A.* **74**, 4777-4780
- Chance, N., Legallais, V., Sorge, J. & Graham, N. (1975a) *Anal. Biochem.* **66**, 498-514
- Chance, B., Graham, N. & Legallais, V. (1975b) *Anal. Biochem.* **67**, 552-579
- Chance, B., Saronio, C. & Leigh, J. S. (1975c) *Proc. Natl. Acad. Sci. U.S.A.* **72**, 1635-1640
- Chance, B., Saronio, C. & Leigh, J. S. (1975d) *J. Biol. Chem.* **250**, 9226-9237
- Chance, B., Leigh, J. S. & Warren, A. (1977) *BBA Libr.* **14**, 1-10
- Clore, G. M. & Chance, E. M. (1978) *Biochem. J.* **173**, 811-820
- Curtis, A. R. (1976) *A.E.R.E. Rep. No. C.S.S. 26*, A.E.R.E., Harwell
- Curtis, A. R. & Chance, E. M. (1972) *A.E.R.E. Rep. No. T.P. 502*, A.E.R.E., Harwell
- Curtis, A. R. & Kirby, C. R. (1977) *A.E.R.E. Rep. No. C.S.S. 46*, A.E.R.E., Harwell
- Denis, M. (1977) *FEBS Lett.* **84**, 296-298
- Erecinska, M., Chance, B. & Wilson, D. F. (1971) *FEBS Lett.* **16**, 284-286
- Falk, K.-E., Vanngård, T. & Angström, J. (1977) *FEBS Lett.* **75**, 23-27
- Gear, C. W. (1971) *Commun. ACM* **14**, 176-179
- Griffiths, D. E. & Wharton, D. C. (1961) *J. Biol. Chem.* **236**, 1850-1862

- Lemberg, M. R. (1969) *Physiol. Rev.* **49**, 48–121
 Lindsay, J. G. & Wilson, D. F. (1974) *FEBS Lett.* **48**, 45–49
 Lindsay, J. G., Owen, C. S. & Wilson, D. F. (1975) *Arch. Biochem. Biophys.* **169**, 492–505
 Low, H. & Vallin, I. (1963) *Biochim. Biophys. Acta* **69**, 361–374
 Mackay, L. N., Kuwana, T. & Hartzell, C. R. (1973) *FEBS Lett.* **36**, 326–329
 Malkin, R. & Malmström, B. G. (1970) *Adv. Enzymol. Relat. Areas Mol. Biol.* **33**, 177–244
 Palmer, G., Babcock, G. T. & Vickery, L. E. (1976) *Proc. Natl. Acad. Sci. U.S.A.* **73**, 2206–2210
 Powell, M. J. D. (1965) *Comput. J.* **7**, 303–307
 Powell, M. J. D. (1972) *A.E.R.E. Rep. No. T.P. 492*, A.E.R.E., Harwell
 Thomson, A. J., Brittain, T., Greenwood, C. & Springall, J. P. (1976) *FEBS Lett.* **67**, 94–98
 Thomson, A. J., Brittain, T., Greenwood, C. & Springall, J. P. (1977) *Biochem. J.* **165**, 327–336
 Van Gelder, B. F. (1963) *Biochim. Biophys. Acta* **73**, 663–665
 Van Gelder, B. F. & Beinert, H. (1969) *Biochim. Biophys. Acta* **189**, 1–24
 Wever, R., Van Drooge, J. H., Muijsers, A. O., Bakker, E. P. & Van Gelder, B. F. (1977) *Eur. J. Biochem.* **73**, 149–154
 Wharton, D. C. & Tzagaloff, A. (1963) *Biochem. Biophys. Res. Commun.* **13**, 121–125
 Wharton, D. C. & Tzagaloff, A. (1964) *J. Biol. Chem.* **239**, 2036–2041
 Wikström, M. K. F., Harmon, H. J., Ingledew, W. J. & Chance, B. (1976) *FEBS Lett.* **65**, 259–277
 William-Smith, D. L., Bray, R. C., Barter, M. J., Tsoponakis, A. D. & Vincent, S. P. (1977) *Biochem. J.* **167**, 593–600
 Wilson, D. F. & Leigh, J. S. (1972) *Arch. Biochem. Biophys.* **150**, 154–163
 Wilson, D. F., Erecinska, M. & Lindsay, J. G. (1975) in *Electron Transfer Chains and Oxidative Phosphorylation* (Quagliariello, E., Papa, S., Palmieri, F., Slater, E. C. & Siliprandi, N., eds.), pp. 69–74, Elsevier/North-Holland, Amsterdam

APPENDIX 1

The experimental data are digitized by using a semi-automatic X-Y reader on the basis of the following mathematical method.

Looking at each curve, we observe that, over a short length (H), the curvature is small. So imagine a regression line fitted to the length H , say:

$$y = ax + b \quad (1)$$

The true regression line would be:

$$y = a_0x + b_0 \quad (2)$$

The residuals in the length H are:

$$r_j = y_j - (ax_j + b) \quad (3)$$

instead of:

$$r_{0j} = y_j - (a_0x_j + b_0) \quad (4)$$

as they should be. Assuming that r_{0j} is Gaussian with mean zero and variance σ^2 , we construct the polynomials (P_i) orthogonal on the points x_j (see later for choice of x_j):

$$P_0(x) = 1 \quad (5)$$

$$P_1(x) = x - \frac{1}{J} \sum x_j \quad (6)$$

(where J is the number of points in the interval H)

$$\begin{aligned} P_2(x) &= (x - \alpha_2)P_1(x) - \beta_2P_0(x) \\ &= \sum_j P_1(x_j)P_2(x_j) \\ &= \sum_j x_j P_1^2(x_j) - \alpha_2 \sum_j P_1^2(x_j) \end{aligned} \quad (7)$$

$$\therefore \alpha_2 = \frac{\sum_j x_j P_1^2(x_j)}{\sum_j P_1^2(x_j)} \quad (8)$$

Now:

$$\begin{aligned} O &= \sum_j P_0(x_j)P_2(x_j) \\ &= \sum_j P_1(x_j) + \frac{1}{J} \sum_j (x_j - \alpha_2)P_1(x_j) - \beta_2 \sum_j P_0^2(x_j) \\ &= \sum_j P_1^2(x_j) - J\beta_2 \end{aligned} \quad (9)$$

$$\therefore \beta_2 = \frac{1}{J} \sum_j P_1^2(x_j) \quad (10)$$

We define:

$$\begin{aligned} R &= \sum_j r_j P_2(x_j) \\ &= \sum_j r_{0j} P_2(x_j) \end{aligned} \quad (11)$$

because P_2 is orthogonal to the straight-line difference. Then:

$$E(R^2) = \sum_j P_2^2(x_j) \sigma^2 \left(\frac{J-2}{J} \right) \quad (12)$$

because two degrees of freedom have to be taken from J in fitting the true regression:

$$\therefore \sigma^2 = \frac{J}{J-2} R^2 \left/ \sum_j P_2^2(x_j) \right. \quad (13)$$

The choice of x_j must satisfy the following conditions: there must be enough of them (say $J \geq 10$); they must be fairly uniformly distributed in the interval H ; they must be chosen without reference to the peaks and troughs of the noise.

To obtain the true regression line ($y = a_0x + b_0$)

from the fitted one ($y = ax + b$) we proceed as follows.

Let:

$$x_j = jh \quad (14)$$

(where h is the interval between x_{j+1} and x_j) and:

$$r_{0j} = y_j - \alpha_0 P_1(x_j) - \beta_0 P_0(x_j) \quad (15)$$

We define:

$$Y_0 = \sum y_j P_0(x_j) \\ = \sum y_j \quad (16)$$

$$Y_1 = \sum y_j P_1(x_j) \quad (17)$$

Then, since for the true regression:

$$O = \sum r_{0j} P_0(x_j) \\ = \sum r_{0j} P_1(x_j) \quad (18)$$

We have

$$Y_0 = \beta_0 \sum P_0^2(x_j) \\ = J\beta_0 \quad (19)$$

$$Y_1 = \alpha_0 \sum P_1^2(x_j) \\ = \frac{J(J+1)(J-1)}{n} h^2 \alpha_0 \quad (20)$$

$$\therefore \alpha_0 = n Y_1 / [J(J^2 - 1)h^2] \quad (21)$$

$$\beta_0 = Y_0 / J \quad (22)$$

The variance (V) of the fitted value at x is then:

$$V = E[(\alpha_0 P_1(x) + \beta_0 P_0(x) - y(x))]^2 \quad (23)$$

where $y(x)$ is the 'true unknown value'. By the ordinary theory:

$$V = P_1^2(x) \text{Var}(\alpha_0^2) + 2P_1(x)P_0(x) \text{Covar}(\alpha_0 \beta_0) + \\ P_0^2(x) \text{Var}(\beta_0^2) \\ = \left(\frac{P_0^2(x)}{J} + \frac{nP_1(x)}{J(J^2-1)h^2} \right) \frac{\sum r_{0j}^2}{J-2} \quad (24)$$

The mean variance (\bar{V}) for $x = 0$ to Jh is:

$$\bar{V} = \frac{1}{(J-1)h} \int_0^{(J-1)h} V dx \\ = \frac{\sum r_{0j}^2}{J(J-2)} \left(1 + \frac{J-1}{J+1} \right) \\ = \frac{2 \sum r_{0j}^2}{(J+1)(J-2)} \quad (25)$$

The square root of \bar{V} is the standard error of the curve. The fractional error in the estimation of the

standard errors of the individual spectroscopic curves, assuming a Gaussian distribution, is given by $1/(2m_i - 2)^{\frac{1}{2}}$, where m_i is the number of data points for curve i . The fractional error in the estimation of the overall standard error of the data is given by the weighted mean of the fractional errors of the individual curves, $\Sigma[m_i/(2m_i - 2)^{\frac{1}{2}}] / \Sigma m_i$.

APPENDIX 2

The s.d._{in} of the ratio or product of two optimized parameters is calculated as follows. Let ψ_i be the s.d._{in} of k_i , ψ_j be the s.d._{in} of k_j , r be the correlation coefficient relating k_i to k_j and α and β be dimensionless constants of value ± 1 . Then $(\alpha \ln k_i + \beta \ln k_j)$ has a s.d. of $(\alpha^2 \psi_i^2 + 2r\alpha\beta\psi_i\psi_j + \beta^2 \psi_j^2)^{\frac{1}{2}}$ and so $(k_i^\alpha k_j^\beta)$ has this s.d._{in}. Thus, in general, if the correlation coefficient of two unknown parameters computed from the variance-covariance matrix, is greater than 0.9 or smaller than -0.9, the ratio or product respectively of the two parameters may be determined even though their individual s.d._{in} may not, provided that these latter are of the same order of magnitude.

APPENDIX 3

The derivation of the expected value of 1 for the correlation index C if the residuals R_i are normal with mean zero and the same variance σ^2 is as follows. The correlation index C is given by:

$$C = \sum R_i / (\sum R_i^2)^{\frac{1}{2}}$$

Consider the expected root-mean-square value of C , $[E(c^2)]^{\frac{1}{2}}$, where:

$$E(c^2) = E[(\sum R_i)^2 / \sum R_i^2]$$

Now:

$$E[(\sum R_i)^2] = m\sigma^2$$

and:

$$E[\sum R_i^2] = m\sigma^2$$

where m is the number of degrees of freedom. So we conclude that $E(c^2) \simeq 1$ and so $[E(c^2)]^{\frac{1}{2}} \simeq 1$.